Universidade de Vigo

Analysis of Time and Space Harmonics in Symmetrical Multiphase Induction Motor Drives by Means of Vector Space Decomposition

Author: Jano Malvar Alvarez
Supervisors: Jesus Doval Gandoy and Oscar Lopez Sanchez

Dissertation submitted for the degree of Doctor of Philosophy at the University of Vigo,
International Doctor Mention

26th, Nov 2015 - Vigo, Spain

APET Applied Power Electronics Technology Research Group

Outline

APET Applied Power Electronics Technology Research Group

Outline

1. Introduction
   - Symmetrical Multiphase Induction Motor
   - Vector Space Decomposition
   - Time and Spatial Harmonics
   - Objectives
2. Vector Space Analysis of Time Harmonics
3. Effects of Spatial Harmonics
4. Conclusions and Future Research

Symmetrical Multiphase Induction Motor

Stator winding with more than three phases ($n > 3$)

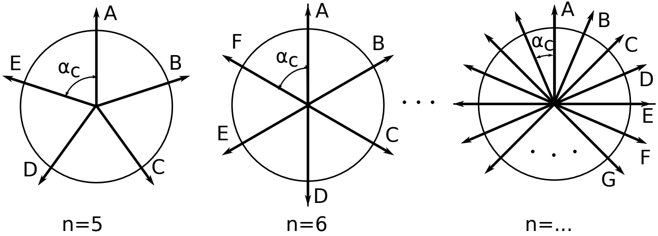

Advantages

- Lower current stress of each power device.
- Reduced harmonics in the DC link.
- Fault tolerance.

APET Applied Power Electronics Technology Research Group

Multiphase Motor Model

Universal Theory of Electric Machines Model:

$$[v^{s}] = [R^{s}][i^{s}] + [L^{ss}]\frac{d}{dt}[i^{s}] + \frac{d}{dt}[L^{sr}][i^{r}]$$
$$[v^{r}] = [R^{r}][i^{r}] + [L^{rr}]\frac{d}{dt}[i^{r}] + \frac{d}{dt}[L^{rs}][i^{s}]$$

Model Assumptions:

- Sinusoidal stator windings.
- Rotor MMF equivalent to the stator one.
- Uniform airgap.
- Neglected magnetic saturation.

Vector Space Decomposition (VSD)

$$\begin{bmatrix} v_1^s \\ v_2^s \\ \vdots \\ v_n^s \end{bmatrix} = [R^s][i^s] + \begin{bmatrix} L_{11}^s & L_{12}^s & \dots & L_{1n}^s \\ L_{21}^s & L_{22}^s & \dots & L_{2n}^s \\ \vdots & \vdots & \ddots & \vdots \\ L_{n1}^s & L_{n2}^s & \dots & L_{nn}^s \end{bmatrix} \frac{d}{dt} \begin{bmatrix} i_1^s \\ i_2^s \\ \vdots \\ i_n^s \end{bmatrix} + \frac{d}{dt} \begin{bmatrix} L_{11}^{sr} & L_{12}^{sr} & \dots & L_{1n}^{sr} \\ L_{21}^{sr} & L_{22}^{sr} & \dots & L_{2n}^{sr} \\ \vdots & \vdots & \ddots & \vdots \\ L_{n1}^{sr} & L_{n2}^{sr} & \dots & L_{nn}^{sr} \end{bmatrix} \begin{bmatrix} i_1^r \\ i_2^r \\ \vdots \\ i_n^r \end{bmatrix}$$

$\Downarrow$ Vector space decomposition

$$\left.\begin{aligned} \mathbf{v}^s_{\alpha\beta}]_0 &= \left(\mathbf{R}^s_{\alpha\beta}]_0 + \mathbf{L}^{ss}_{\alpha\beta}]_0 \tfrac{d}{dt}\right)\mathbf{i}^s_{\alpha\beta}]_0 + \dots \\ &\vdots \\ \mathbf{v}^s_{\alpha\beta}]_p &= \left(\mathbf{R}^s_{\alpha\beta}]_p + \mathbf{L}^{ss}_{\alpha\beta}]_p \tfrac{d}{dt}\right)\mathbf{i}^s_{\alpha\beta}]_p + \dots \\ &\vdots \\ \mathbf{v}^s_{\alpha\beta}]_{n-1} &= \left(\mathbf{R}^s_{\alpha\beta}]_{n-1} + \mathbf{L}^{ss}_{\alpha\beta}]_{n-1} \tfrac{d}{dt}\right)\mathbf{i}^s_{\alpha\beta}]_{n-1} + \dots \end{aligned}\right\} \text{Orthogonal decoupled subspaces.}$$

Th. 7-9

APET Applied Power Electronics Technology Research Group

VSD of the Multiphase Model

Stationary model

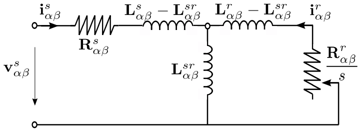

α-β plane

- Electromechanical energy conversion.

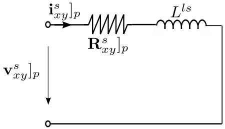

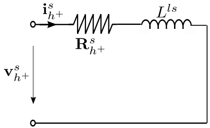

x-y plane

h homopolar axis

- No-torque.
- Low impedance.
- Extra losses.

Voltage and Current Mapping

Component mapping: identification of the subspace of each spatial vector.

Uses:

- Components that affect torque production.
- Components that only produce losses.
- Current harmonic control.

Previous works:

- Focused on specific numbers of phases.
- n-phase studies that only cover the α-β plane.

Control of Multiphase Induction Motors

Torque and flux: controlled by the current components in α-β.

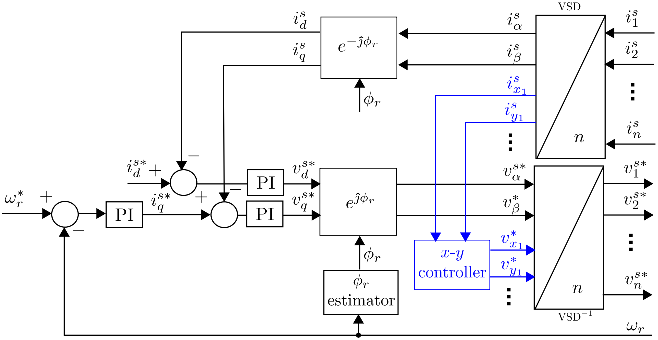

Applications of the additional degrees of freedom:

- Fault tolerance.
- Series connected multimotor drives.

APET Applied Power Electronics Technology Research Group

Series-Connected Multimotor Drives

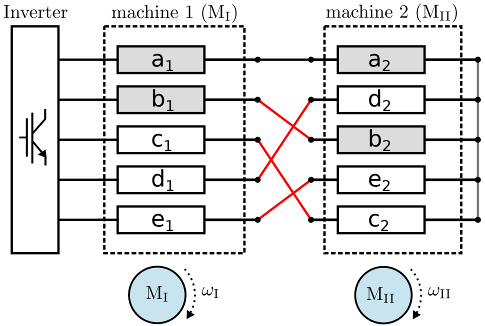

Independent control a set of motors fed from a single converter.

- Requires a physical phase transposition.

$$v^* = \underbrace{\widehat{v}_{\mathrm{I}} \sin\left(\omega_{\mathrm{I}} t + \eta\alpha_c\right)}_{v^*_{\mathrm{M_I}}} + \underbrace{\widehat{v}_{\mathrm{II}} \sin\left(\omega_{\mathrm{II}} t + \eta 2\alpha_c\right)}_{v^*_{\mathrm{M_{II}}}}$$

Phase order affects how the current and voltage components are mapped.

Th. 12-15

Harmonic Analysis in *n*-Phase Motors

Multiphase IM model: harmonic analysis limitations.

Extended Motor Model:
Flux density produced by one phase:

$$B(\theta, t) = \frac{\mu}{2g} \int K(\theta) \cdot i(t) d\theta$$

- $i(t)$: current.
- $K(\theta)$: winding distribution.
- g: airgap.
- μ: magnetic permeability.

In 3-phase machines, this equation has been used to evaluate:

- Time harmonics.
- Distribution harmonics.
- Permeance harmonics.

Th.
16,17

Time Harmonics

$$B(\theta, t) = \frac{\mu}{2g} \int K(\theta) \cdot \boxed{i(t)}\, d\theta$$

Time harmonics: harmonics in the electrical signals.

Causes:

- Converter deadtime.
- Voltage drops on power devices.
- DC link variations.
- Motor non-linearities.

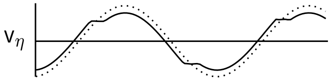

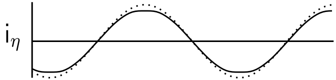

$$v_\eta = \sum_{q=3,5,7,\ldots} \widehat{v}_{\eta,q} \cdot \cos(q(\omega_s t - \eta\alpha_c) + \phi_q)$$

$$i_\eta = \sum_{q=3,5,7,\ldots} \widehat{i}_{\eta,q} \cdot \sin\left(q(\omega_s t - \eta\alpha_c) + \phi_q\right)$$

q: time harmonic order.

Th. 15, 16

APET Applied Power Electronics Technology Research Group

Distribution Harmonics

$$B(\theta, t) = \frac{\mu}{2g} \int \boxed{K(\theta)} \cdot i(t) d\theta$$

Distribution harmonics: due to the spatial conductor distribution.

Causes:

- Non-sinusoidal conductor distributions.
- Finite number of slots.

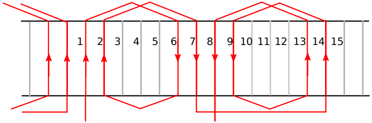

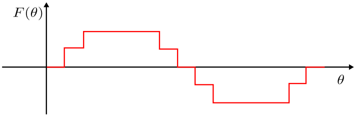

$$K_\eta(\theta) = \sum_{\nu=1}^{\infty} \widehat{K}_{\eta,\nu} \cos\left(\nu(P\theta - \eta\alpha_c) + \phi_\nu\right)$$

ν: distribution harmonic order.

Th.
17-19

APET Applied Power Electronics Technology Research Group

Magnetic Permeance Harmonics

$$B(\theta, t) = \frac{1}{2}\boxed{\frac{\mu}{g}}\int K(\theta) \cdot i(t) d\theta$$

Harmonics due to non-linearities in the **magnetic permeance:** $\Lambda(\theta, t) = \mu/g$.

Causes:

- Non-uniform airgap.
- Magnetic saturation.

Th.
21, 22

Magnetic Permeance Harmonics

$$B(\theta, t) = \frac{1}{2}\boxed{\frac{\mu}{g}} \int K(\theta) \cdot i(t) d\theta$$

Harmonics due to non-linearities in the **magnetic permeance:** $\Lambda(\theta, t) = \mu/g$.

- Slotting permeance harmonics:

$$\Lambda_{slt} = \sum_{k_s=0}^{\infty} \sum_{k_r=0}^{\infty} \frac{1}{2}\widehat{\Lambda}_{rs} \Big(\cos\left(k_s Q_s \theta + k_r Q_r(\theta - \theta_{\mathrm{r}})\right) + \cos\left(k_s Q_s \theta - k_r Q_r(\theta - \theta_{\mathrm{r}})\right)\Big).$$

Causes:

- Non-uniform airgap.
- Magnetic saturation.

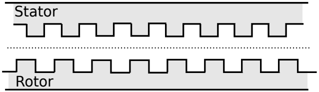

Th.
21, 22

Magnetic Permeance Harmonics

$$B(\theta, t) = \frac{1}{2}\boxed{\frac{\mu}{g}}\int K(\theta)\cdot i(t)d\theta$$

Causes:

- Non-uniform airgap.
- Magnetic saturation.

Harmonics due to non-linearities in the **magnetic permeance:** $\Lambda(\theta, t) = \mu/g$.

- Slotting permeance harmonics:

$$\Lambda_{slt} = \sum_{k_s=0}^{\infty}\sum_{k_r=0}^{\infty}\frac{1}{2}\widehat{\Lambda}_{rs}\Big(\cos\left(k_s Q_s\theta + k_r Q_r(\theta-\theta_{\mathrm{r}})\right) + \cos\left(k_s Q_s\theta - k_r Q_r(\theta-\theta_{\mathrm{r}})\right)\Big).$$

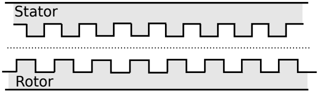

- Flux saturation permeance harmonics:

$$\Lambda_{\rho} = \sum_{\rho=1}^{\infty}\frac{1}{2}\widehat{\Lambda}_{\rho}\cos\left[2\rho(P\theta - \omega_s t)\right]$$

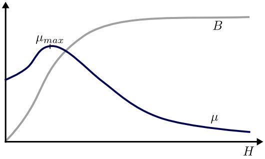

Th.
21, 22

Characterization of Current Harmonics

Flux Density harmonics $\Longrightarrow$ Induced current components

Modeling the induced current harmonics is important for:

- Current harmonic cancellation.
- Torque ripple control.
- Sensorless speed measurement.
- Fault detection.

Previous induced current harmonic characterizations:

- Mainly focused on 3-phase machines.
- n-phase works: uniform airgap and negligible saturation.
- Only frequency identification.

Th. 26-28

Motor Current Signature Analysis

The motor current signature analysis is a fault detection technique based on:

- **Healthy motor current signature**: Identification and classification of the stator current harmonics in the healthy motor.
- **Symptom**: current harmonics produced by a specific motor fault.

It has been used to detect:

- Stator winding faults.
- Broken rotor bars.
- Rotor eccentricity.

MCSA Eccentricity Detection

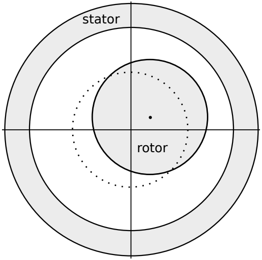

Eccentricity types:

- Static
- Dynamic
- Mixed

Static eccentricity permeance function:

$$\Lambda_{se} = \sum_{k_{se}=1}^{\infty} \widehat{\Lambda}_{k_{se}} \cos\left(k_{se}\theta\right)$$

Dynamic eccentricity permeance function:

$$\Lambda_{de} = \sum_{k_{de}=1}^{\infty} \widehat{\Lambda}_{k_{de}} \cos\left(k_{de}(\theta - \omega_r t)\right)$$

Th.
22, 23

APET Applied Power Electronics Technology Research Group

Previous Eccentricity Detection Methods

Classic 3-phase eccentricity fault symptoms:

- Fundamental current sidebands.
  - Only for dynamic or mixed eccentricities.
- For static eccentricities: Principal slot harmonics (PSHs).
  - Valid only for $Q_r = P(3k \pm 1)$..

Complementary static eccentricity detection methods (3-phase):

- Zero sequence current $\longrightarrow$ requires a neutral connection.
- Flux harmonics $\longrightarrow$ requires additional sensors.
- Negative sequence $\longrightarrow$ low symptom amplitude.

Eccentricity detection in multiphase motors is not as broadly researched as in 3-phases.

Th. 28,29

Applied Power Electronics Technology Research Group

Summary of Previous Research Limitations

Harmonic mapping in multiphase motors:

- Specific number of phases only or *n*-phase analysis centered in the α-β plane.
- Multimotor drives suggested that physical phase order affects mapping.
- Previous works do not evaluate these phase order effects.

Th. 28,29

Applied Power Electronics Technology Research Group

Summary of Previous Research Limitations

Harmonic mapping in multiphase motors:

- Specific number of phases only or *n*-phase analysis centered in the α-β plane.
- Multimotor drives suggested that physical phase order affects mapping.
- Previous works do not evaluate these phase order effects.

Previous works about current signature:

- Mainly focused only on 3-phase motors.
- *n*-phase works: uniform airgap and negligible saturation.
- Only frequency characterization.
- Eccentricity detection in multiphase motors is an under-researched topic.

Th. 28,29

Main Objectives of this Thesis

Analysis of time and space harmonics in symmetrical multiphase induction motor drives by means of vector space decomposition.

- Time harmonic analysis (Chapter 2):
  - Method for identifying the SV mapping subspace and rotating speed that evaluates harmonic order and phase sequence.
- Extension of the method for spatial harmonics (Chapter 3):
  - Include the harmonics due to: conductor distribution, non-uniform airgap and magnetic saturation.
  - Study the healthy n-phase motor current signature.
  - Investigate the MCSA eccentricity detection in n-phase IM.

Th. 28,29

Outline

Th.
28,29

APET Applied Power Electronics Technology Research Group

Introduction: Previous Concepts

- Multiphase IM model original reference frame $\Rightarrow$ cross-coupled variables.
- VSD: transformation proposed to decouple variables.
- VSD $\Rightarrow$ α-β and x-y planes and h axes.
- Time harmonics: harmonics in the electrical signals (i.e. voltage and current).
- Applications of time harmonic mapping:
  - Components that affect torque production.
  - Components that only produce losses.
  - Current harmonic control.

Th.
34, 35

Introduction: objectives of this chapter

Objectives:

- Time harmonic analysis in symmetrical multiphase machines by means of VSD.
- Method for identifying the SV mapping subspace and rotating speed that evaluates harmonic order and phase sequence.
- Validated through an experimental setup.

Th.
34, 35

Multiphase Voltage VSD

Voltage harmonics: $V_\eta = \sum_q \widehat{v}_{\eta,q} \cdot \cos[q(\omega_s t - \eta\alpha_c) + \phi_q]$

$\Downarrow$ Vector space decomposition.

$$\mathbf{V}_{p,q} = \widehat{v}_{\eta,q} \cdot \left[\mathbf{A}^{+}_{p,q} \cdot e^{\hat{\jmath}(q\omega_s t+\phi_q)} + \mathbf{A}^{-}_{p,q} \cdot e^{\hat{\jmath}(-q\omega_s t-\phi_q)}\right]$$

$$\mathbf{A}^{+}_{p,q} = \begin{cases} n \text{ if } e^{\hat{\jmath}q\alpha_c}=e^{\hat{\jmath}p\alpha_c} \\ 0 \text{ if } e^{\hat{\jmath}q\alpha_c}\neq e^{\hat{\jmath}p\alpha_c} \end{cases} \qquad \mathbf{A}^{-}_{p,q} = \begin{cases} n \text{ if } e^{\hat{\jmath}q\alpha_c}=e^{\hat{\jmath}(-p)\alpha_c} \\ 0 \text{ if } e^{\hat{\jmath}q\alpha_c}\neq e^{\hat{\jmath}(-p)\alpha_c} \end{cases}$$

Positive rotation direction: defined by the fundamental SV.

$e^{\hat{\jmath}q\alpha_c} = e^{\hat{\jmath}p\alpha_c}$	Positive rotating SV.
$e^{\hat{\jmath}q\alpha_c} = e^{\hat{\jmath}(-p)\alpha_c}$	Negative rotating SV.

Th. 36-38

TIME HARMONIC MAPPING DIAGRAM

$$e^{\hat{j}q\alpha_c} = e^{\hat{j}p\alpha_c}$$
$$e^{\hat{j}q\alpha_c} = e^{\hat{j}(-p)\alpha_c} \quad \Leftarrow \quad \begin{aligned} q &= 1, 2, 3, \ldots \\ p &= \underbrace{0}_{h^+}, \underbrace{1, \ldots, n/2-1}_{\alpha_p\text{-}\beta_p}, \underbrace{n/2}_{h^-}\} \end{aligned}$$

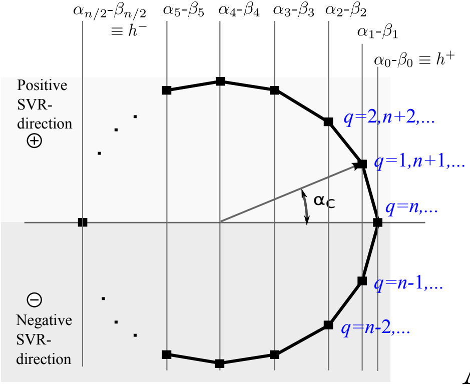

Th. 39-41

APET Applied Power Electronics Technology Research Group

Harmonic Mapping Example: 5-Phase Motor

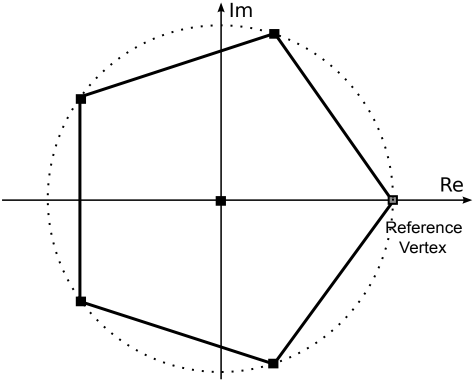

Applied Power Electronics Technology Research Group

Harmonic Mapping Example: 5-Phase Motor

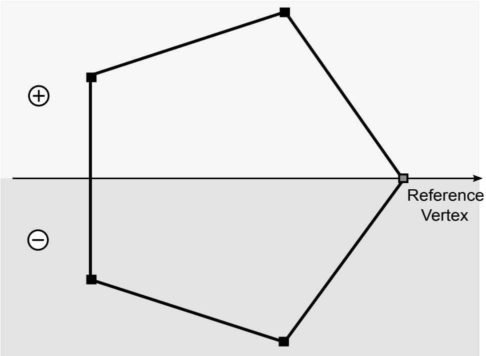

Th.
39-43

Harmonic Mapping Example: 5-Phase Motor

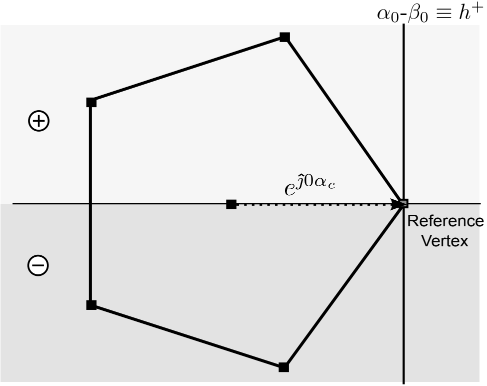

$$e^{\hat{\jmath}q\alpha_c} = \boxed{e^{\hat{\jmath}p\alpha_c}}$$

$$e^{\hat{\jmath}q\alpha_c} = \boxed{e^{\hat{\jmath}(-p)\alpha_c}}$$

Th.
39-43

Harmonic Mapping Example: 5-Phase Motor

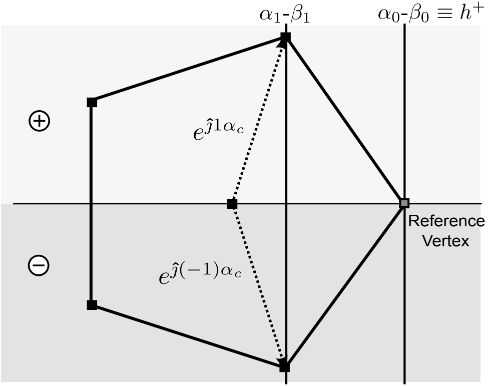

$$e^{\hat{\jmath}q\alpha_c} = e^{\hat{\jmath}p\alpha_c}$$

$$e^{\hat{\jmath}q\alpha_c} = e^{\hat{\jmath}(-p)\alpha_c}$$

Th. 39-43

APET Applied Power Electronics Technology Research Group

Harmonic Mapping Example: 5-Phase Motor

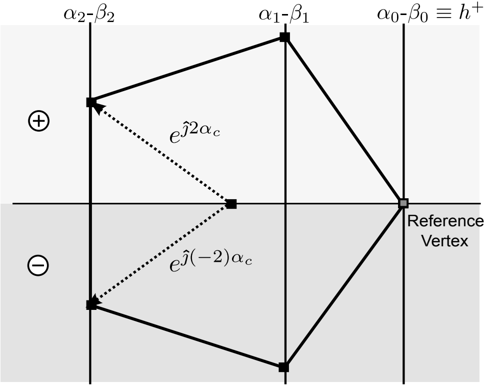

$$e^{\hat{\jmath}q\alpha_c} = e^{\hat{\jmath}p\alpha_c}$$

$$e^{\hat{\jmath}q\alpha_c} = e^{\hat{\jmath}(-p)\alpha_c}$$

Th. 39-43

Harmonic Mapping Example: 5-Phase Motor

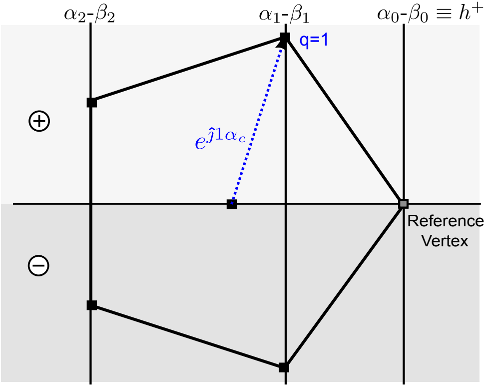

$$e^{\hat{\jmath} q \alpha_c} = e^{\hat{\jmath} p \alpha_c}$$

$$e^{\hat{\jmath} q \alpha_c} = e^{\hat{\jmath} (-p) \alpha_c}$$

Th. 39-43

APET Applied Power Electronics Technology Research Group

Harmonic Mapping Example: 5-Phase Motor

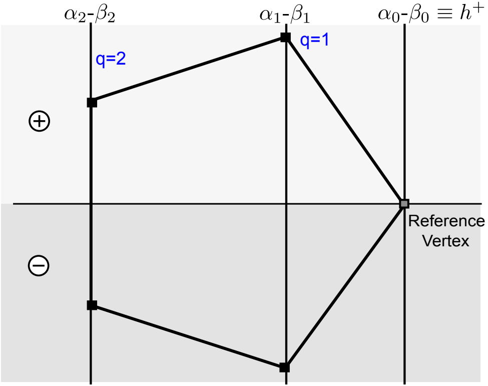

$$e^{\hat{\jmath} q \alpha_c} = e^{\hat{\jmath} p \alpha_c}$$

$$e^{\hat{\jmath} q \alpha_c} = e^{\hat{\jmath} (-p) \alpha_c}$$

Th.
39-43

APET Applied Power Electronics Technology Research Group

Harmonic Mapping Example: 5-Phase Motor

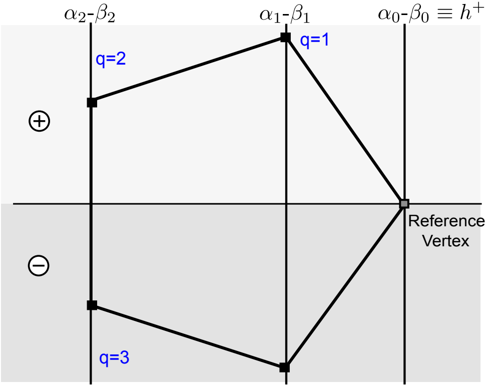

$$e^{\hat{\jmath} q \alpha_c} = e^{\hat{\jmath} p \alpha_c}$$

$$e^{\hat{\jmath} q \alpha_c} = e^{\hat{\jmath} (-p) \alpha_c}$$

Th.
39-43

APET Applied Power Electronics Technology Research Group

Harmonic Mapping Example: 5-Phase Motor

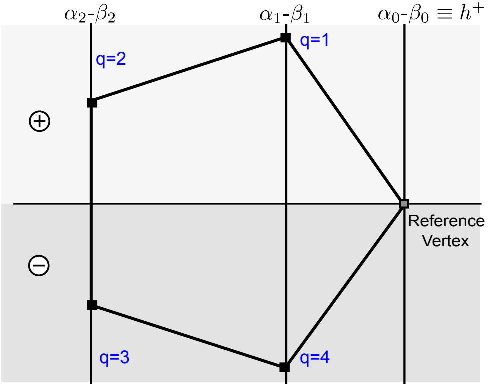

$$e^{\hat{j}q\alpha_c} = e^{\hat{j}p\alpha_c}$$

$$e^{\hat{j}q\alpha_c} = e^{\hat{j}(-p)\alpha_c}$$

Th. 39-43

Harmonic Mapping Example: 5-Phase Motor

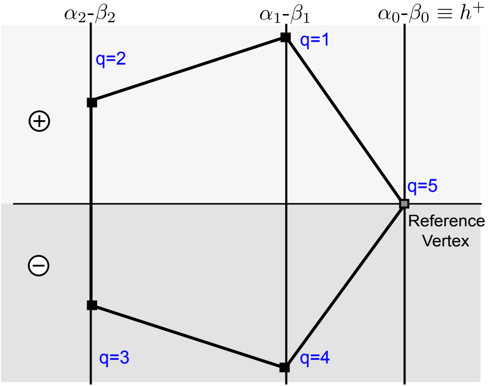

$$e^{\hat{\jmath} q \alpha_c} = e^{\hat{\jmath} p \alpha_c}$$

$$e^{\hat{\jmath} q \alpha_c} = e^{\hat{\jmath}(-p) \alpha_c}$$

Th.
39-43

HARMONIC MAPPING EXAMPLE: 5-PHASE MOTOR

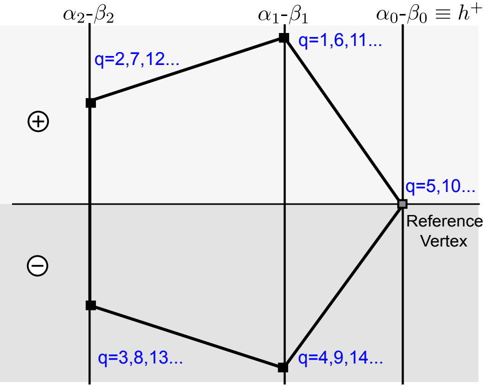

SVR direction	α_1-β_1	α_2-β_2	h^+
+	$q = 1, 6, 11, \ldots$	$q = 2, 7, 12, \ldots$	$q = 5, 10, \ldots$
-	$q = 4, 9, 14, \ldots$	$q = 3, 8, 13, \ldots$	

Th.
39-43

PHASE SEQUENCE INFLUENCE ON MAPPING

PHYSICAL PHASE TRANSPOSITION

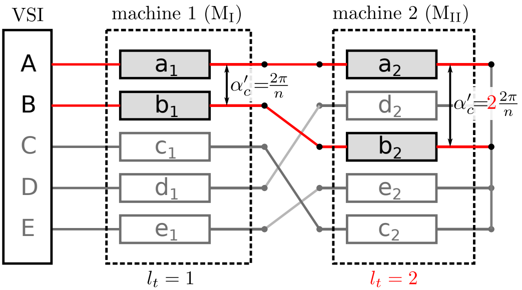

$$\alpha_c' = l_t\, \alpha_c$$

l_t: physical phase transposition step.

- Mapping equations:

$$e^{\hat{\jmath} q \alpha_c} = e^{\hat{\jmath} p l_t \alpha_c}$$

$$e^{\hat{\jmath} q \alpha_c} = e^{\hat{\jmath} (-p) l_t \alpha_c}$$

Th. 39-43

APET Applied Power Electronics Technology Research Group

Phase Sequence Influence on Mapping

Reference Delay Angle

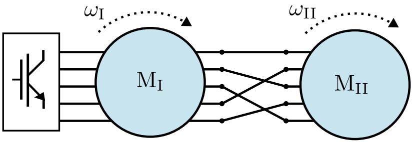

$$v^* = \underbrace{\hat{v}_{\mathrm{I}} \sin\left(\omega_{\mathrm{I}} t + \eta\alpha_c\right)}_{v^*_{\mathrm{M_I}}} + \underbrace{\hat{v}_{\mathrm{II}} \sin\left(\omega_{\mathrm{II}} t + \eta 2\alpha_c\right)}_{v^*_{\mathrm{M_{II}}}}$$

m: reference delay angle step.

- Mapping equations:

$$e^{\hat{\jmath} q m \alpha_c} = e^{\hat{\jmath} p \alpha_c}$$

$$e^{\hat{\jmath} q m \alpha_c} = e^{\hat{\jmath}(-p) \alpha_c}$$

EXAMPLE: 5-5 MULTIMOTOR DRIVE

MAPPING OF v_I^* HARMONICS IN M_I.

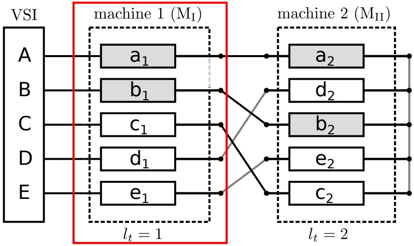

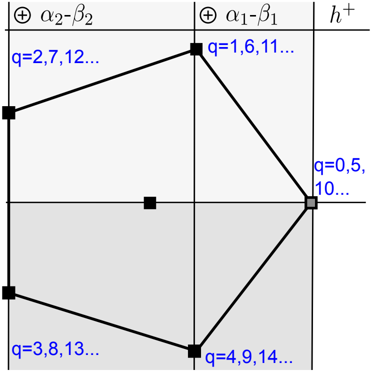

$$v^* = \widehat{v}_I \sin(\omega_I t + \eta\alpha_c)$$
$$+\widehat{v}_{II} \sin(\omega_{II} t + \eta 2\alpha_c)$$

$$e^{\hat{\jmath}q\,\alpha_c} = e^{\hat{\jmath}p\,\alpha_c}$$
$$e^{\hat{\jmath}q\,\alpha_c} = e^{\hat{\jmath}(-p)\,\alpha_c}$$

Example: 5-5 Multimotor Drive

Mapping of v_I^* harmonics in M_{II}.

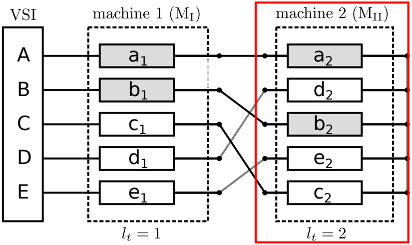

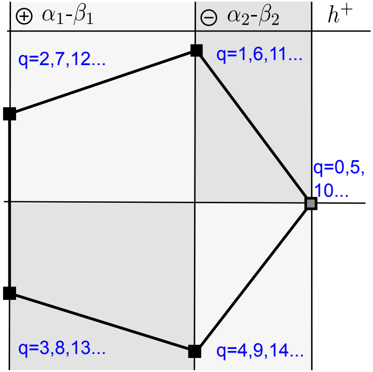

$$v^* = \widehat{v}_{\mathrm{I}} \sin\left(\omega_{\mathrm{I}} t + \eta \alpha_c\right) + \widehat{v}_{\mathrm{II}} \sin\left(\omega_{\mathrm{II}} t + \eta 2 \alpha_c\right)$$

$$e^{\hat{\jmath} q\, \alpha_c} = e^{\hat{\jmath} p 2 \alpha_c}$$

$$e^{\hat{\jmath} q\, \alpha_c} = e^{\hat{\jmath}(-p) 2 \alpha_c}$$

Example: 5-5 Multimotor Drive

Mapping of v^*_{II} harmonics in M_I.

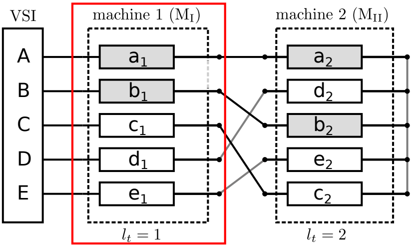

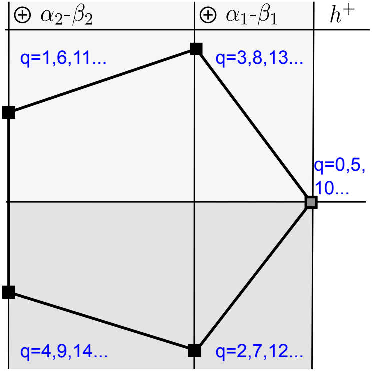

$$v^* = \widehat{v}_{I} \sin\left(\omega_{I} t + \eta\alpha_c\right) + \widehat{v}_{II} \sin\left(\omega_{II} t + \eta 2\alpha_c\right)$$

$$e^{\jmath q 2\alpha_c} = e^{\jmath p\, \alpha_c}$$

$$e^{\jmath q 2\alpha_c} = e^{\jmath (-p)\, \alpha_c}$$

EXAMPLE: 5-5 MULTIMOTOR DRIVE

MAPPING OF v^*_{II} HARMONICS IN M_{II}.

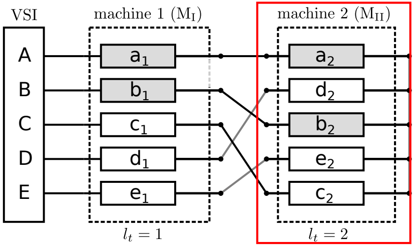

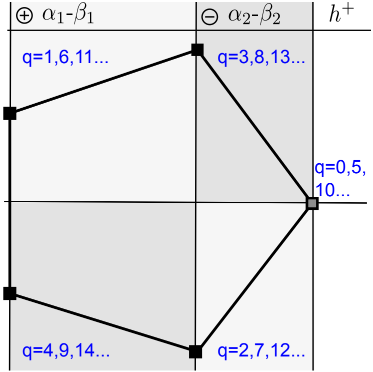

$$v^* = \widehat{v}_I \sin(\omega_I t + \eta\alpha_c)$$
$$+ \widehat{v}_{II} \sin(\omega_{II} t + \eta 2\alpha_c)$$

$$e^{\hat{j}q2\alpha_c} = e^{\hat{j}p2\alpha_c}$$
$$e^{\hat{j}q2\alpha_c} = e^{\hat{j}(-p)2\alpha_c}$$

Th. 36

APET Applied Power Electronics Technology Research Group

Experimental Setup

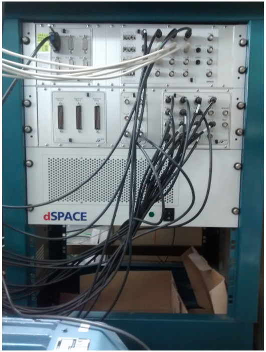

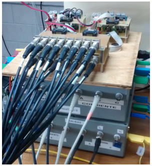

- 2x Semikron Semistack SKS 35F
- dSPACE DS1006
- LEM LV 25-P
- LEM LA 55-P
- Apicom FR5ME
- $V_{DC} = 300\ \mathrm{V}$
- $f_s = 10\ \mathrm{kHz}$

APET Applied Power Electronics Technology Research Group

Five-Phase Single Motor Drive

Voltage and Current VSD Spectrum

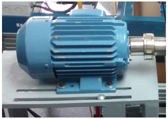

$$v^* = \sum_{q=1}^{12} A_l^* \cos q(\omega_l^* t - \eta\alpha_c)$$

Predicted mapping from the diagram:

SVR direction	α_1-β_1	α_2-β_2	h^+
+	$q = 1, 6, 11$	$q = 2, 7, 12$	$q = 5, 10$
-	$q = 4, 9$	$q = 3, 8$	

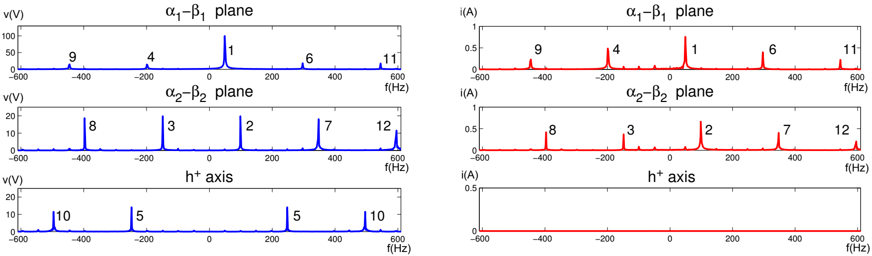

The experimental results corroborate the 5-phase IM mapping predicted by the diagram.

Th. 49-51

APET Applied Power Electronics Technology Research Group

Five-Phase Single Motor Drive

Delay Angle Step m Experiment

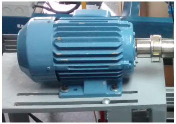

$$V_\eta^* = \widehat{v}_\eta^* \cos(\omega_s t - m\eta\alpha_c)$$

Predicted mapping:

$m = 1$	α-β	Torque
$m = 2$	x-y	Low impedance
$m = 3$		No torque
$m = 4$	α-β	Torque
$m = 5$	h^+	No current

Results:

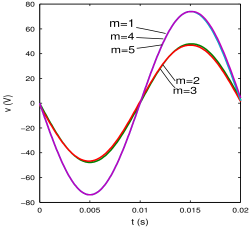

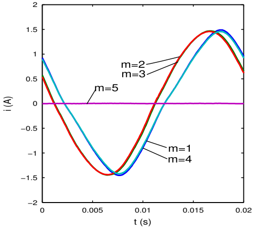

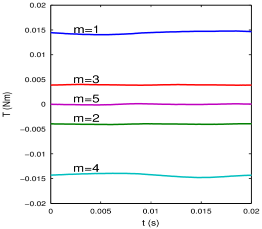

Results corroborate the predicted effects of m in the harmonic mapping.

Th. 49-51

APET Applied Power Electronics Technology Research Group

Five-Phase Single Motor Drive

Delay Angle Step *m* Experiment

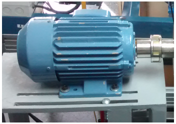

$$V_\eta^* = \hat{v}_\eta^* \cos(\omega_s t - m\eta\alpha_c)$$

Predicted mapping:

$m = 1$	α-β	Torque
$m = 2$	x-y	Low impedance
$m = 3$		No torque
$m = 4$	α-β	Torque
$m = 5$	h^+	No current

Results:

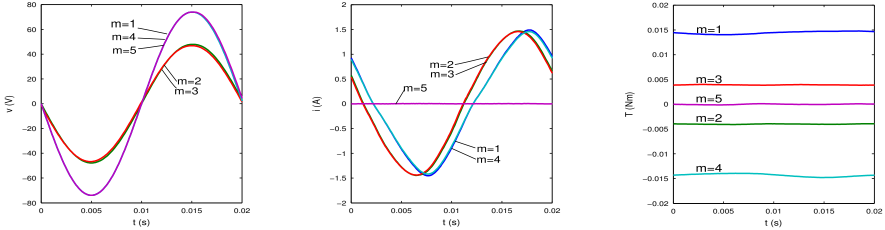

Results corroborate the predicted effects of *m* in the harmonic mapping.

Th. 49-51

APET Applied Power Electronics Technology Research Group

Series-Connected Six-Phase Two-Motor Drive

Experimental setup

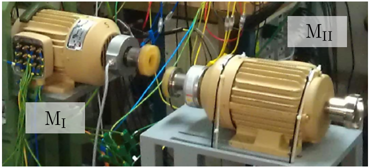

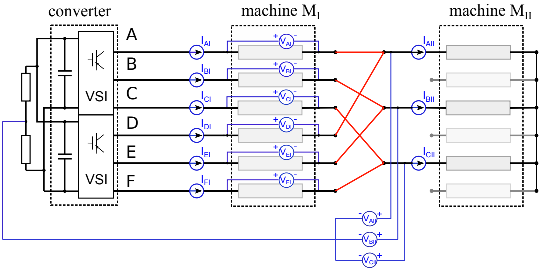

$$V_\eta^* = \underbrace{A_I^* \cos\left(\omega_I^* t - \eta\alpha_c\right)}_{[V]_I^*} + \underbrace{A_{II}^* \cos\left(\omega_{II}^* t - 2\eta\alpha_c\right)}_{[V]_{II}^*}$$

Th. 56

Series-Connected Six-Phase Two-Motor Drive

M_I Harmonics Mapping in M_I and M_{II}

$$V_\eta^* = A_I^* \cos(\omega_I^* t - \eta\alpha_c) + A_{II}^* \cos(\omega_{II}^* t - 2\eta\alpha_c) + \sum_{q=2}^{12} A_I^* \cos q(\omega_I^* t - \eta\alpha_c)$$

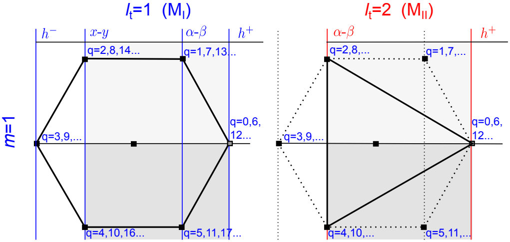

Th. 57,58

Series-Connected Six-Phase Two-Motor Drive

M_I Harmonics Mapping in M_I and M_{II}

$$V^*_\eta = A^*_I \cos(\omega^*_I t - \eta\alpha_c) + A^*_{II}\cos(\omega^*_{II} t - 2\eta\alpha_c) + \sum_{q=2}^{12} A^*_I \cos q(\omega^*_I t - \eta\alpha_c)$$

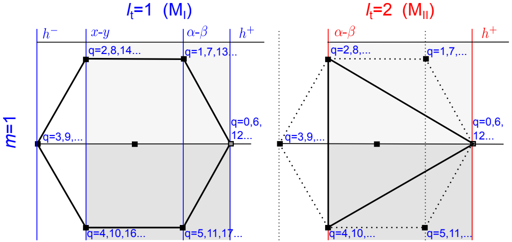

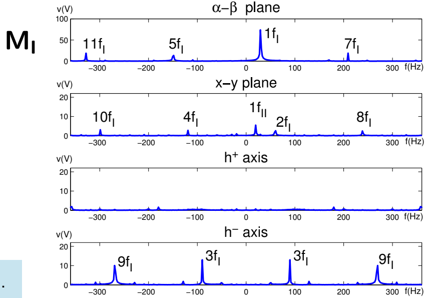

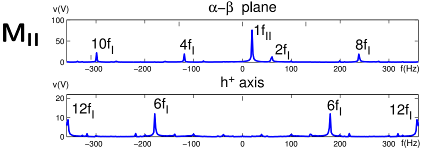

Th. 57,58

APET Applied Power Electronics Technology Research Group

Series-Connected Six-Phase Two-Motor Drive

M_{II} Harmonics Mapping in M_I and M_{II}

$$V_\eta^* = A_I^* \cos(\omega_I^* t - \eta\alpha_c) + A_{II}^* \cos(\omega_{II}^* t - 2\eta\alpha_c) + \sum_{q=2}^{12} A_{II}^* \cos q(\omega_{II}^* t - 2\eta\alpha_c)$$

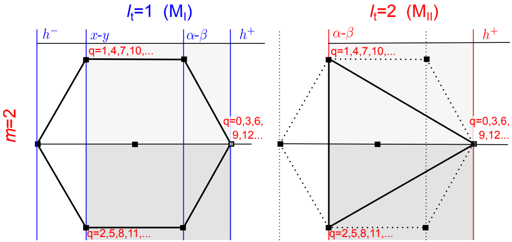

Th. 57-59

Series-Connected Six-Phase Two-Motor Drive

M_{II} Harmonics Mapping in M_I and M_{II}

$$V^*_\eta = A^*_I \cos(\omega^*_I t - \eta\alpha_c) + A^*_{II} \cos(\omega^*_{II} t - 2\eta\alpha_c) + \sum_{q=2}^{12} A^*_{II} \cos q(\omega^*_{II} t - 2\eta\alpha_c)$$

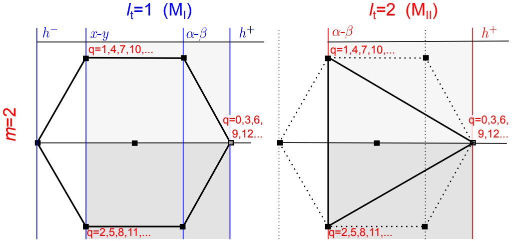

M_I

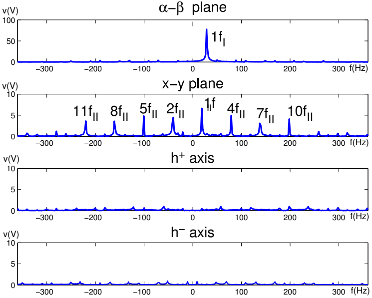

M_{II}

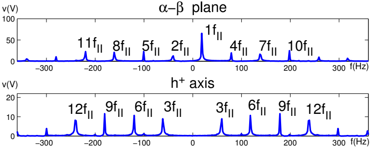

Results corroborate the harmonic mapping predicted by the diagram.

Th. 57-59

Conclusion of This Chapter

- A study of time harmonic mapping in symmetrical *n*-phase motors that takes into account the effects of a physical angle transposition or a delay angle step.
- Simple graphical mapping method has been proposed.
- Experimentally tests on a single-motor and a series-connected multimotor drive.

Outline

APET Applied Power Electronics Technology Research Group

Introduction: Previous Concepts

- Time and spatial harmonics.
- Spatial harmonics:
  - Distribution of conductors.
  - Magnetic saturation.
  - Non-uniform airgap.
- Characterization of the spatial harmonics interests:
  - Motor understanding.
  - Current control.
  - Sensorless.
  - MCSA.
- MCSA methods for rotor eccentricity detection in 3-phase motors:
  - Monitoring the fundamental current sidebands.
  - Monitoring the PSHs.

Th.
74, 75

Introduction: objectives of this chapter

Objectives:

- Extension of the VSD analysis to spatial harmonics, including:
  - Conductor distribution.
  - Non-uniform airgap.
  - Magnetic saturation.
- Study the healthy *n*-phase motor current signature.
- Investigate the MCSA eccentricity detection in *n*-phase IM.

Multiphase Harmonic Analysis

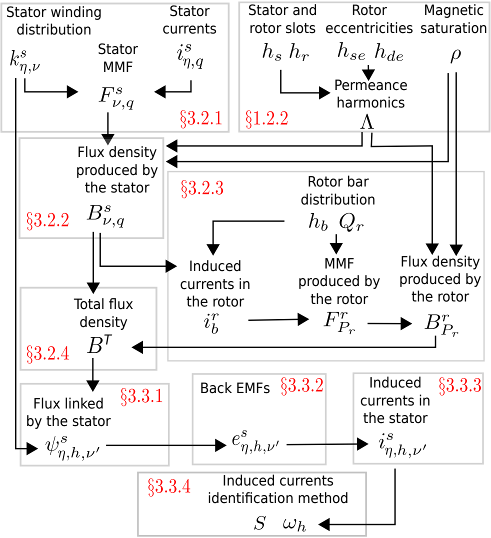

Th. 76

APET Applied Power Electronics Technology Research Group

MULTIPHASE HARMONIC ANALYSIS

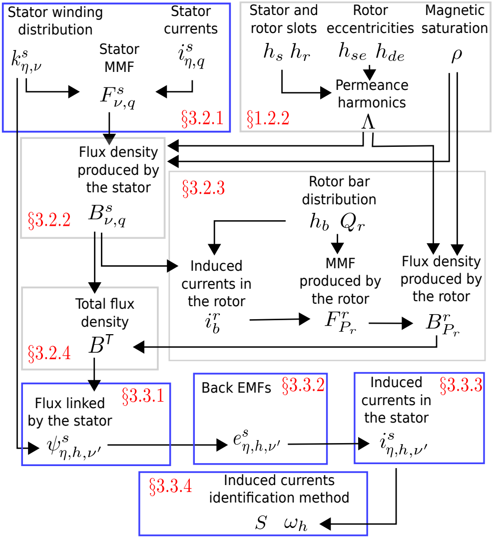

n-phase specific:

- Stator MMF
- Flux linked by the stator
- Back-EMFs
- Induced currents
- Current harmonic mapping

Induced Currents in the Multiphase Stator

Analyzed harmonics:

- Converter.
- Stator and rotor conductor distribution.
- Stator and rotor slots.
- Magnetic saturation.

Stator Induced Current Harmonics:

$$i^{s}_{\eta,h,\nu'} = \widehat{i}^{s}_{\eta,h,\nu'} \cos\left(\omega_h t - \nu' \eta \alpha_c + \phi_\psi - \phi_{\eta,\nu'}\right)$$

$$\omega_h = k_r Q_r \omega_r + k_\rho q \omega_s$$

$$\nu' = \frac{P_h}{P} = kn + k_\rho q + k_s \frac{Q_s}{P} + k_r \frac{Q_r}{P}$$

Th. 86-88

Induced Currents in the Multiphase Stator

Stator Induced Current Harmonics:

$$i^{s}_{\eta,h,\nu'} = \widehat{i}^{s}_{\eta,h,\nu'} \cos\left(\omega_h t - \nu'\eta\alpha_c + \phi_\psi - \phi_{\eta,\nu'}\right)$$

$$\omega_h = k_r Q_r \omega_r + k_\rho q \omega_s$$

$$\nu' = \frac{P_h}{P} = kn + k_\rho q + k_s \frac{Q_s}{P} + k_r \frac{Q_r}{P}$$

- k_r, k_s: rotor and stator slot harmonic order.
- k_ρ: magnetic saturation harmonic order.
- $\frac{P_h}{P}$: flux harmonic equivalent pole pairs.

Flux harmonics generate induced currents only if $\nu' = \frac{P_h}{P}$.

Th. 86-88

APET Applied Power Electronics Technology Research Group

Induced Current Harmonic Mapping

$$i^{s}_{\eta,h,\nu'} = \widehat{i}^{s}_{\eta,h,\nu'} \cos\left(\omega_h t - \nu' \eta \alpha_c + \phi_\psi - \phi_{\eta,\nu'}\right)$$

- ω_h: frequency.
- $\nu' = \frac{P_h}{P}$: mapping.

ν': equivalent to m in time harmonics.

Mapping equations:

$$e^{\hat{\jmath}\nu'\alpha_c} = e^{\hat{\jmath}p\alpha_c}$$

$$e^{\hat{\jmath}\nu'\alpha_c} = e^{\hat{\jmath}(-p)\alpha_c}$$

Mapping diagram ($n = 5$):

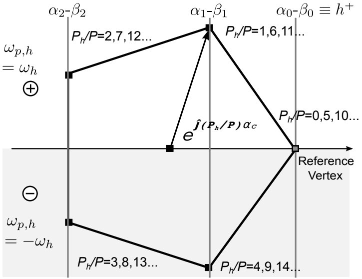

Th. 88-91

Induced Current Harmonics Example

Five-Phase Integral Slot Motor

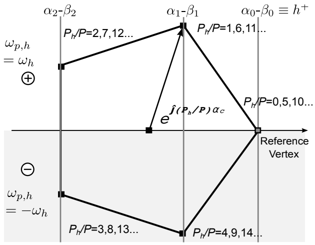

$$\frac{P_h}{P} = kn + k_\rho q + k_s \frac{Q_s}{P} + k_r \frac{Q_r}{P}$$

n=5, *P*=2, *Qr*=22 and *Qs*=30					
qk_ρ	k_s/P	k_r/P	$\omega_{p,h}$	P_h/P	Subspace
1	0	0	ω_s	1	$\alpha - \beta$
		1	$22\omega_r+\omega_s$	12	$x - y$
		-1		-10	h_+
		2	$-44\omega_r-\omega_s$	23	$x - y$
		-2	$44\omega_r-\omega_s$	-21	$\alpha - \beta$
	⋮				
	1	0	ω_s	16	$\alpha - \beta$
		1	$22\omega_r+\omega_s$	27	$x - y$
		-1		5	h_+
	⋮				
	2	0	ω_s	31	$\alpha - \beta$
	⋮				
3	0	0	$-3\omega_s$	3	$x - y$
		1	$-22\omega_r-3\omega_s$	14	$\alpha - \beta$
		-1	$-22\omega_r+3\omega$	-8	$x - y$
	⋮				
5	0	0		5	h_+
	⋮				
7	0	0	$7\omega_s$	7	$x - y$
	⋮				
⋮					

Th. 89-91

Induced Current Harmonics Example

Five-Phase Integral Slot Motor

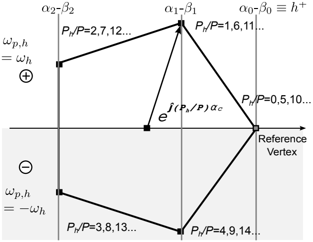

$$\frac{P_h}{P} = kn + k_\rho q + k_s \frac{Q_s}{P} + k_r \frac{Q_r}{P}$$

n=5, *P*=2, *Qr*=22 and *Qs*=30

qk_ρ	k_s/P	k_r/P	$\omega_{p,h}$	P_h/P	Subspace
1	0	0	ω_s	1	α – β
		1	$22\omega_r+\omega_s$	12	$x-y$
		-1		-10	h_+
		2	$-44\omega_r-\omega_s$	23	$x-y$
		-2	$44\omega_r-\omega_s$	-21	α – β
	⋮				
	1	0	ω_s	16	α – β
		1	$22\omega_r+\omega_s$	27	$x-y$
		-1		5	h_+
	⋮				
	2	0	ω_s	31	α – β
	⋮				
3	0	0	$-3\omega_s$	3	$x-y$
		1	$-22\omega_r-3\omega_s$	14	α – β
		-1	$-22\omega_r+3\omega$	-8	$x-y$
	⋮				
5	0	0		5	h_+
	⋮				
7	0	0	$7\omega_s$	7	$x-y$
	⋮				
⋮					

Th. 89-91

Induced Current Harmonics Example

Five-Phase Integral Slot Motor

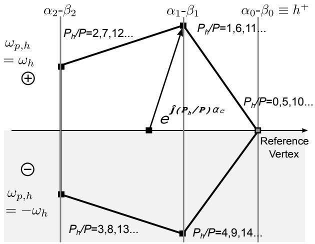

$$\frac{P_h}{P} = kn + k_\rho q + k_s \frac{Q_s}{P} + k_r \frac{Q_r}{P}$$

n=5, P=2, Qr=22 and Qs=30					
qk_ρ	k_s/P	k_r/P	$\omega_{p,h}$	P_h/P	Subspace
1	0	0	ω_s	1	$\alpha-\beta$
		1	$22\omega_r+\omega_s$	12	$x-y$
		-1		-10	h_+
		2	$-44\omega_r-\omega_s$	23	$x-y$
		-2	$44\omega_r-\omega_s$	-21	$\alpha-\beta$
	⋮				
	1	0	ω_s	16	$\alpha-\beta$
		1	$22\omega_r+\omega_s$	27	$x-y$
		-1		5	h_+
	⋮				
	2	0	ω_s	31	$\alpha-\beta$
	⋮				
3	0	0	$-3\omega_s$	3	$x-y$
		1	$-22\omega_r-3\omega_s$	14	$\alpha-\beta$
		-1	$-22\omega_r+3\omega$	-8	$x-y$
	⋮				
5	0	0		5	h_+
	⋮				
7	0	0	$7\omega_s$	7	$x-y$
	⋮				
⋮					

Th. 89-91

Induced Current Harmonics Example

Five-Phase Integral Slot Motor

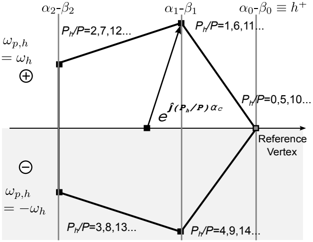

$$\frac{P_h}{P} = kn + k_\rho q + k_s \frac{Q_s}{P} + k_r \frac{Q_r}{P}$$

n=5, P=2, Qr=22 and Qs=30

qk_ρ	k_s/P	k_r/P	$\omega_{p,h}$	P_h/P	Subspace
1	0	0	ω_s	1	$\alpha-\beta$
		1	$22\omega_r+\omega_s$	12	$x-y$
		-1		-10	h_+
		2	$-44\omega_r-\omega_s$	23	$x-y$
		-2	$44\omega_r-\omega_s$	-21	$\alpha-\beta$
	⋮				
	1	0	ω_s	16	$\alpha-\beta$
		1	$22\omega_r+\omega_s$	27	$x-y$
		-1		5	h_+
	⋮				
	2	0	ω_s	31	$\alpha-\beta$
	⋮				
3	0	0	$-3\omega_s$	3	$x-y$
		1	$-22\omega_r-3\omega_s$	14	$\alpha-\beta$
		-1	$-22\omega_r+3\omega$	-8	$x-y$
	⋮				
5	0	0		5	h_+
	⋮				
7	0	0	$7\omega_s$	7	$x-y$
	⋮				
⋮					

Th. 89-91

Current Harmonics Due to Eccentricity

Stator Induced Current Harmonics:

$$i^{s}_{\eta,h,\nu'} = \widehat{i}^{s}_{\eta,h,\nu'} \cos\left(\omega_h t - \nu' \eta \alpha_c + \phi_\psi - \phi_{\eta,\nu'}\right)$$

$$\omega_h = (k_r Q_r + k_{de})\omega_r + k_\rho q \omega_s$$

$$\nu' = \frac{P_h}{P} = kn + k_\rho q + k_s \frac{Q_s}{P} + k_r \frac{Q_r}{P} + \frac{k_{de}}{P} + \frac{k_{se}}{P}$$

- k_{se}: static eccentricity harmonic order.
  - Not new frequencies.
  - Changes mapping subspaces.
- k_{de}: dynamic eccentricity harmonic order.
  - New frequencies appear.
  - Changes mapping subspaces.

Th.
89-91

APET Applied Power Electronics Technology Research Group

Classic MCSA Eccentricity Detection

Adaptation of the Classic Methods to Multiphase Motors

$$\omega_h = (k_r Q_r + k_{de})\omega_r + k_\rho q \omega_s$$
$$\nu' = \frac{P_h}{P} = kn + k_\rho q + k_s \frac{Q_s}{P} + k_r \frac{Q_r}{P} + \frac{k_{de}}{P} + \frac{k_{se}}{P}$$

Fundamental current sidebands:

- Symptom frequency: $\omega_h = |k_{de}\omega_r \pm \omega_s|$, valid for *n*-phase motors.
- No pure static eccentricity detection.

Monitoring PSHs:

- Symptom frequency: $\omega_h = |k_r Q_r \omega_r \pm \omega_s|$.
- Valid in 3-phase motors if $Q_r = P(3k \pm 1)$.

Th. 94-96

PSHs method in *n*-phase motors:

$$Q_r = P(nk \pm 1)$$

VSD MCSA ECCENTRICITY DETECTION METHOD

STATIC ECCENTRICITY SYMPTOM

$$\omega_h = (k_r Q_r + k_{de})\omega_r + k_\rho q \omega_s$$
$$\nu' = \frac{P_h}{P} = kn + k_\rho q + k_s \frac{Q_s}{P} + k_r \frac{Q_r}{P} + \frac{k_{de}}{P} + \frac{k_{se}}{P}$$

Static eccentricity symptom: induced current due to the fundamental component of the flux and static eccentricity.

- Frequency: $\omega_h = \omega_s$
- Pole pairs: $\frac{P_h}{P} = 1 + \frac{k_{se}}{P}$

Advantages:
- Independent from Q_r or P.
- Higher amplitude than PSHs.
- Independent from ω_r (slip).
- Lower frequencies than PSHs.

Th. 96-99

VSD MCSA Eccentricity Detection Method

Dynamic Eccentricity Symptom

$$\omega_h = (k_r Q_r + k_{de})\omega_r + k_\rho q \omega_s$$
$$\nu' = \frac{P_h}{P} = kn + k_\rho q + k_s \frac{Q_s}{P} + k_r \frac{Q_r}{P} + \frac{k_{de}}{P} + \frac{k_{se}}{P}$$

Dynamic eccentricity symptom: induced current due to the fundamental component of the flux and dynamic eccentricity.

- Frequency: $\omega_h = k_{de}\omega_r + \omega_s$
- Pole pairs: $\frac{P_h}{P} = 1 + \frac{k_{de}}{P}$

Pure dynamic eccentricity: no specific advantages.

Th. 96-99

Experimental Setup

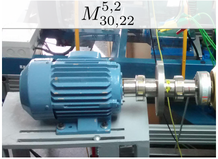

- 0.75 kW
- $n = 5$
- $P = 2$
- $Q_s = 30$
- $Q_r = 22$

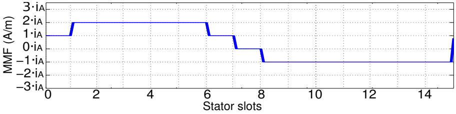

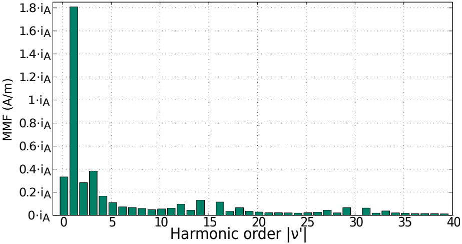

Th. 100,101

APET Applied Power Electronics Technology Research Group

Healthy Current Spectrum of $M^{5,2}_{30,22}$

- Fundamental component: 50 Hz.
- Three values of the slip.

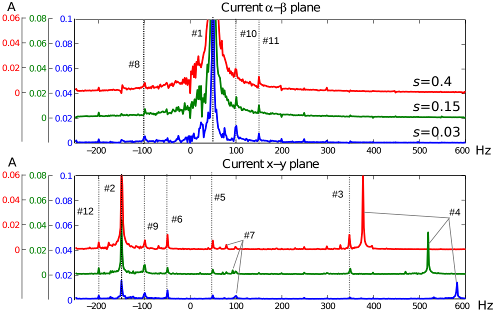

	SVR speed (Hz)			Subspace
	s=0.4	s=0.15	s=0.03	
#1	50	50	50	$\alpha-\beta$
#2	-150	-150	-150	$x-y$
#3	350	350	350	$x-y$
#4	380	517.5	583.5	$x-y$
#5	50	50	50	$x-y$
#6	-50	-50	-50	$x-y$
#7	80	92.5	99	$x-y$
#8	-100	-100	-100	$\alpha-\beta$
#9	-100	-100	-100	$x-y$
#10	100	100	100	$\alpha-\beta$
#11	150	150	150	$\alpha-\beta$
#12	-200	-200	-200	$x-y$

Healthy Current Spectrum of $M^{5,2}_{30,22}$

	SVR speed (Hz)			Subspace	$q k_\rho$	k_s	k_r	k_{se}	k_{de}	
	s=0.4	s=0.15	s=0.03							
#1	50	50	50	$\alpha-\beta$	1	0	0	0	0	Inverter Harm.
#2	-150	-150	-150	$x-y$	3	0	0	0	0	
#3	350	350	350	$x-y$	7	0	0	0	0	
#4	380	517.5	583.5	$x-y$	1	0	1	0	0	Slotting
#5	50	50	50	$x-y$	1	0	0	2	0	Static Ecce.
#6	-50	-50	-50	$x-y$	1	0	0	4	0	
#7	80	92.5	99	$x-y$	1	0	0	0	2	Dynamic
#8	-100	-100	-100	$\alpha-\beta$	2	0	0	-6	0	Mixed Origins
#9	-100	-100	-100	$x-y$	2	0	0	2	0	
#10	100	100	100	$\alpha-\beta$	2	0	0	-2	0	
#11	150	150	150	$\alpha-\beta$	3	0	0	-4	0	
#12	-200	-200	-200	$x-y$	4	0	0	-2	0	

Th. 102-107

The identified frequencies and mapping subspaces coincide with the predicted ones.

Static Eccentricity Experiment

Comparison of the PSHs and the VSD Eccentricity Detection Methods

Static eccentricity tests:

- Test 1: $\alpha_u = 0.00$ rad (black line)
- Test 2: $\alpha_u = 0.02$ rad (green line)
- Test 3: $\alpha_u = 0.04$ rad (blue line)
- Test 4: $\alpha_u = 0.06$ rad (red line)

The imposed eccentricity levels are low $\longrightarrow$ symptom amplitudes are low.

Classic PSHs Method

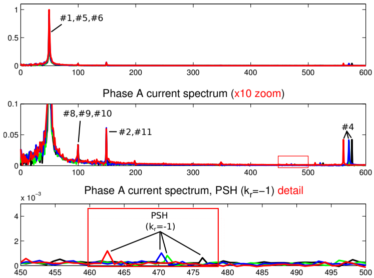

Th. 107-109

APET Applied Power Electronics Technology Research Group

Static Eccentricity Experiment

Comparison of the PSHs and the VSD Eccentricity Detection Methods

Static eccentricity tests:

- Test 1: $\alpha_u = 0.00\,\mathrm{rad}$ (black line)
- Test 2: $\alpha_u = 0.02\,\mathrm{rad}$ (green line)
- Test 3: $\alpha_u = 0.04\,\mathrm{rad}$ (blue line)
- Test 4: $\alpha_u = 0.06\,\mathrm{rad}$ (red line)

Static eccentricity symptom: #6.

VSD Method

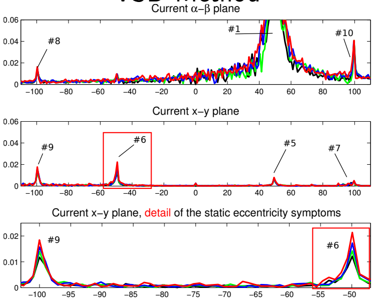

Static Eccentricity Experiment

Comparison of the PSHs and the VSD Eccentricity Detection Methods

Classic PSHs Method

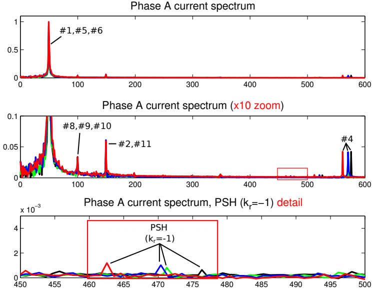

VSD Method

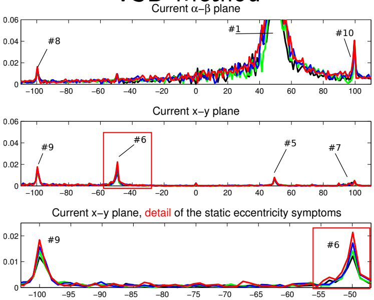

VSD Method Advantages:

Harmonics easier to detect:

- Higher amplitudes.
- Lower frequencies.
- Independent from the slip.

Th. 107-109

APET Applied Power Electronics Technology Research Group

Mixed Eccentricity Experiment

Constant dynamic eccentricity, increase in the static one.

Classic Sidebands Method

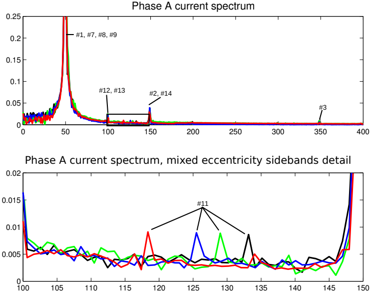

VSD Method

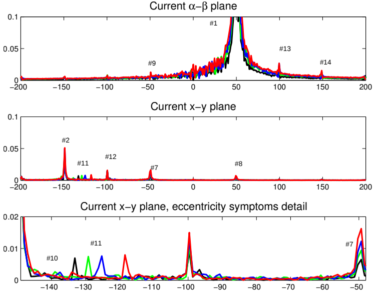

VSD Method Advantages:

- Independent symptoms for the dynamic and static eccentricity: distinguish variations in each one.

Th. 110-113

APET Applied Power Electronics Technology Research Group

Conclusion of This Chapter

- VSD analysis is extended to cover current harmonics due to:
  - Conductor distribution.
  - Non-uniform airgap.
  - Magnetic saturation.
- It is used to analyze the current signature of healthy multiphase squirrel cage motors.
- The application of the classic MCSA eccentricity detection methods to multiphase motors is studied.
- New MCSA eccentricity detection method based on the VSD analysis of the stator current has been proposed.
  - Symptoms have higher amplitudes and lower frequencies.
  - Can be used in the cases the classic method is not valid.
  - Distinguish between static or dynamic eccentricity variations.

OUTLINE

Conclusion

- Study and characterization of time and spatial harmonics in an n-phase induction motor by means of the VSD.
- VSD analysis of time harmonics (Chapter 2):
  - Graphical mapping method.
  - Harmonics mapping in low impedance planes or producing torque ripple.
  - Phase order effects in mapping.
- VSD analysis of spatial harmonics (Chapter 3):
  - Healthy motor current signature study.
  - Classic eccentricity detection MCSA methods.
  - New eccentricity detection method based on the VSD.

APET Applied Power Electronics Technology Research Group

Conclusion

- Study and characterization of time and spatial harmonics in an *n*-phase induction motor by means of the VSD.
- VSD analysis of time harmonics (Chapter 2):
  - Graphical mapping method.
  - Harmonics mapping in low impedance planes or producing torque ripple.
  - Phase order effects in mapping.
- VSD analysis of spatial harmonics (Chapter 3):
  - Healthy motor current signature study.
  - Classic eccentricity detection MCSA methods.
  - New eccentricity detection method based on the VSD.

Th.
115,116

FUTURE RESEARCH

- Extension of the analysis to other type of motors:
  - Asymmetrical multiphase induction motors.
  - Permanent magnet motors.
  - Doubly-fed generators.
- Extension of the proposed MCSA method to other common motor faults, such as: broken rotor bars, bearing faults, gearbox failures, ...
- Application to sensorless speed measurement.

Universidade Vigo

Analysis of Time and Space Harmonics in Symmetrical Multiphase Induction Motor Drives by Means of Vector Space Decomposition

Author: Jano Malvar Alvarez
Supervisors: Jesus Doval Gandoy and Oscar Lopez Sanchez

Dissertation submitted for the degree of Doctor of Philosophy at the University of Vigo, International Doctor Mention

26th, Nov 2015 - Vigo, Spain

Th.
116

APET Applied Power Electronics Technology Research Group